Sādhanā (2019)44:191
https://doi.org/10.1007/s12046-019-1174-1
© Indian Academy of Sciences

Geotechnical stability assessment of a railway arch bridge more than 100-year old: a case study

PRIYANKA GHOSH[1,*], RAJEEV SHRIVASTAVA[2] and ABHIJEET SWAIN[1]

[1]Department of Civil Engineering, Indian Institute of Technology Kanpur, Kanpur 208 016, India
[2]West North Central Railway, Allahabad, India
e-mail: priyog@iitk.ac.in

MS received 25 October 2018; revised 28 May 2019; accepted 16 June 2019

Abstract. In the present investigation, the geotechnical stability of the substructure of 100-year-old brick masonry rail bridges has been analysed numerically in the presence of nearby newly proposed concrete box bridges. Two different arch bridges (1273/1 and 1274/1) of Indian Railways (IR) have been considered in this analysis. Both bridges are made of brick masonry with different numbers of barrels. The numerical analysis has been performed using the finite-element (FE) method. The existing railway track between Kanpur and Jhansi, India, runs on these bridges, which were basically constructed by the British between 1888 and 1900. Therefore, the assessment of geotechnical safety and stability of such heritage bridges was of paramount importance from the IR point of view since the modern rail loading and other associated factors were changed significantly. A detailed geotechnical investigation along with the plate load test was carried out at the respective bridge locations, and the results are reported in this paper. The distribution of the vertical stress and the settlement developed below the foundation of the bridges have been acquired from the FE investigation to judge the foundation safety against the strength and the serviceability perspective.

Keywords. Bearing capacity; foundation interaction; geotechnical investigation; railway arch bridge; settlement.

1. Introduction

The railway is considered to be one of the major transportation facilities in several countries and India is not an exception. The Indian Railways (IR) is one of the oldest railway organizations over the globe, which was initiated by the British in 1853. In India, the railways provide the least expensive and most advantageous method of passenger transport both for long distance and suburban traffic. It has played a significant role in the development and the growth of the country by evacuating separation amongst the urban areas and the countryside, and has assumed a noteworthy part in spreading developments and new thoughts. The IR has advanced a great deal, both qualitatively and quantitatively, during the last few decades. To continue with the growth, the IR recently decided to lay down 204 km long second railway track next to the current track between Bhimsen Junction (26.4195°N, 80.2177°E) near Kanpur Central (26.4539°N, 80.3512°E) and Jhansi Junction (25.4452°N, 78.5527°E) railway stations (figure 1). Kanpur Central is one of the five "Central" railway stations in India, which is the busiest railway station in the state Uttar Pradesh in terms of the frequency of trains. Kanpur Central is a major intercity rail and commuter rail station in the city of Kanpur and is located on the Howrah–Delhi broad gauge route passing through Uttar Pradesh. Being the busiest station of the North Central Railways, Kanpur Central accommodates around 372 trains and traffic of more than 7,50,000 passengers daily, while Jhansi Junction is a major railway junction in the city of Jhansi in Bundelkhand region of Uttar Pradesh, which is one of the busiest and largest railway stations in India. Jhansi Junction is a significant intercity hub and a technical stoppage for many superfast trains in India, which lies on the main Delhi–Chennai and Delhi–Mumbai rail route. Being an old rail network in the world, the IR apparently owns several old heritage structures such as bridges and buildings. Therefore, it has been a significant challenge for the IR to maintain the well-being of such heritage structures while accommodating the modernization. The existing track between Kanpur Central and Jhansi Junction is such an old route, which was laid down by the British between 1888 and 1900. Due to the topography, the existing track (figure 1) keeps running over several brick masonry arch bridges, which were constructed by the British more than 100 years ago. Thereafter the loading applied on the railway tracks has been changed to a great extent due to the modernization of the railway facilities. With the

*For correspondence
Published online: 03 August 2019

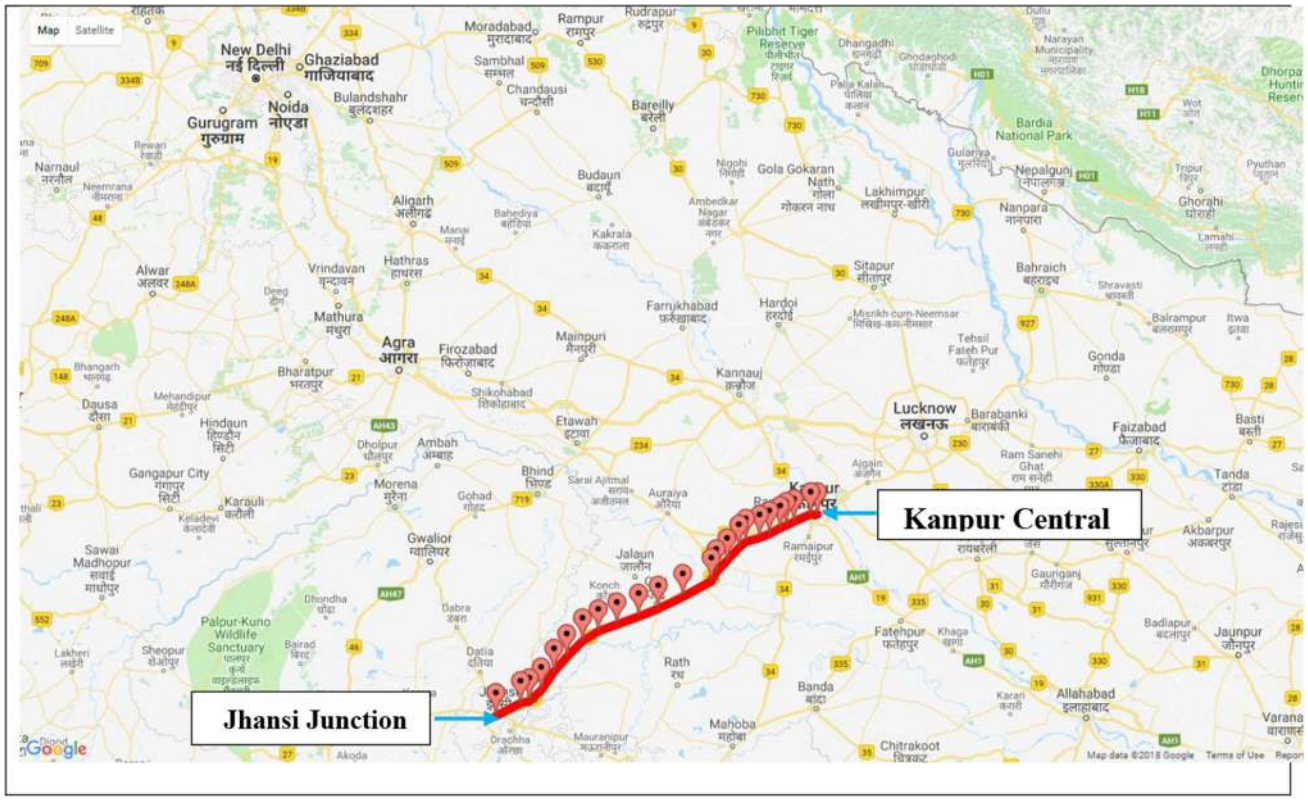

Figure 1. Existing railway track between Kanpur Central and Jhansi Junction (source: http://www.onefivenine.com/india/Rail/RailDetails/54158).

enhancement in the rail loading, only the visual distress of such old railway bridges used to be monitored by the IR to identify the requirement of any rehabilitation process such as the generic reinforced cement concrete (RCC) jacketing of the bridges. With the proposed doubling of the railway track between Bhimsen Junction and Jhansi Junction, the new track is planned to keep running over the concrete box bridges constructed adjacent to the existing old bridges. Hence, a need was felt to investigate the geotechnical safety and stability of the substructure of the existing old heritage bridges due to the construction of the adjacent newly proposed concrete box bridges [1]. Besides, the IR also planned to enhance the applied live load (train load) on the existing as well as the proposed tracks. Therefore, a significant amount of interaction was expected to happen between the foundations of the old and the new bridges. The interaction effect of closely spaced foundations has been studied by several researchers [2–14], where it has been demonstrated that the bearing capacity of the interacting foundations generally gets enhanced at the cost of a higher settlement. Therefore, in the present study, the geotechnical stability of the existing old bridges in terms of the vertical stress and the settlement developed below the foundation has been explored in the presence of the newly proposed bridges. For the sake of brevity, out of several such old arch bridges, only two bridges (1273/1 and 1274/1) have been considered in this paper. Bridge 1273/1 is made of brick masonry with three barrels as shown in figure 2a, whereas bridge 1274/1 is made of brick masonry with two barrels as shown in figure 2b. It can be seen from figure 2 that both bridges carry a significant height of an earth cushion on the top of the superstructure. In this study, the vertical stress and the settlement developed at the base of the existing bridge in the presence of the proposed bridge have been determined using the finite-element (FE) analysis [15]. The present investigation is purely based on a case study that has assessed the geotechnical stability of railway bridges in India more than 100 years old under the enhanced rail loading and the changed site conditions.

2. Geotechnical investigation and plate load test

Geotechnical investigations were carried out at the respective bridge locations, which included the scope of detailed subsoil investigation and the plate load test. The subsoil investigation included field exploration, in-situ testing and collection of the soil samples, laboratory testing and analysis of the test results. A borehole 150 mm in diameter and 15 m in depth was drilled at each bridge location. For the advancement of the boreholes at the selected locations, the percussion drilling technique was

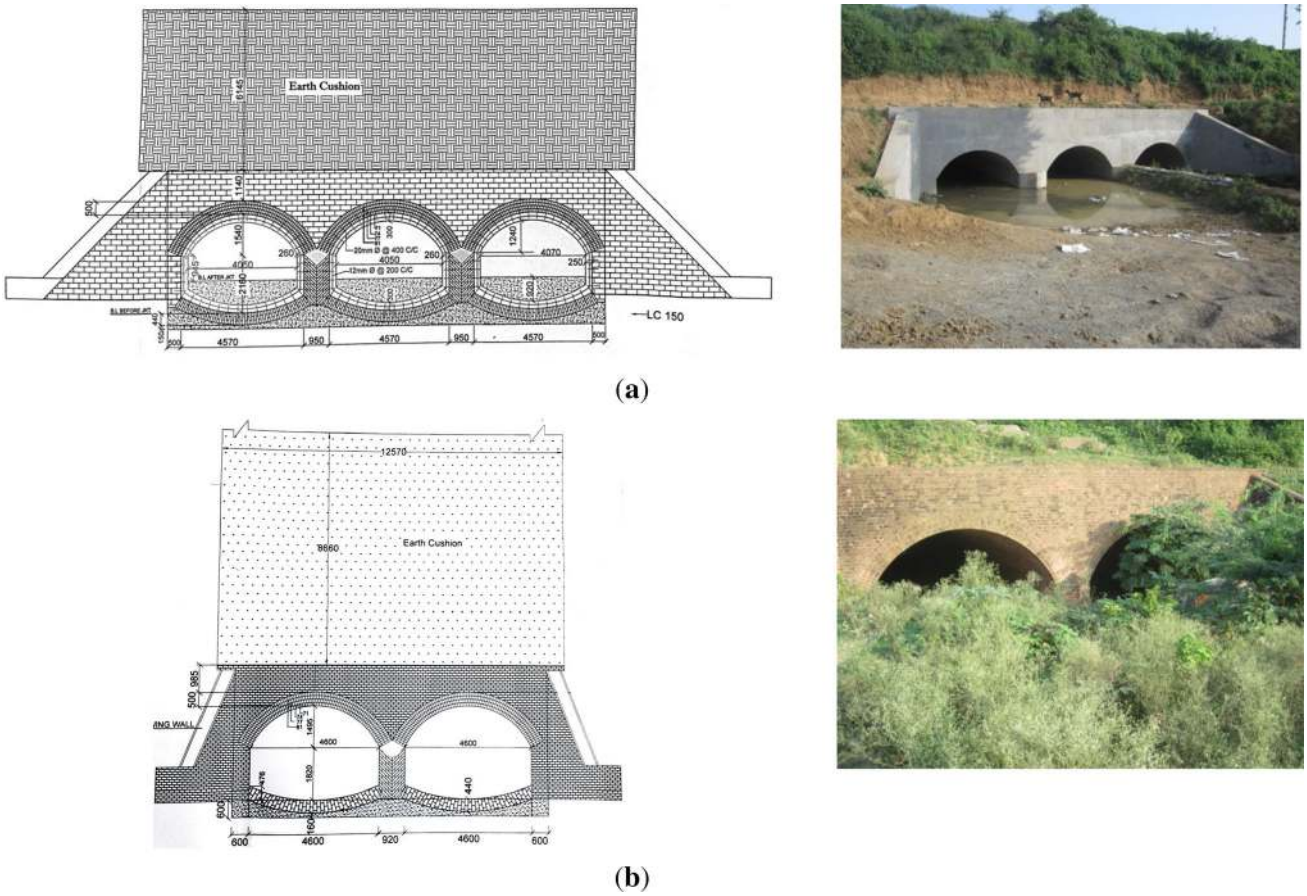

Figure 2. Sectional elevation details of the existing bridge: (**a**) 1273/1 and (**b**) 1274/1 (all dimensions are in mm) (modified after RVNL).

adopted. Disturbed and undisturbed soil samples representing various subsoil layers encountered were collected. The disturbed soil samples were used for the identification and the classification purpose, whereas the undisturbed samples were used for the evaluation of the strength and the compressibility properties of the soil. With the advancement of the boreholes, standard penetration tests (SPT) were performed at regular intervals in each of the boreholes as per the procedure stipulated in the Indian standard specification [16], and eventually, the N values were recorded at each stage. Soil samples collected from the field were brought to conduct various laboratory tests to determine different soil parameters [17]. For different bridge locations, the bore-log data and the classification of soil as per the IS classification system at different depths are given in figure 3. From the bore-log data presented in figure 3a, the subsurface soil layers at the location of bridge 1273/1 are generally found to be medium plastic silty clay (CL-CI) or low to medium silt (ML-MI) depending upon the presence of the silt content throughout the explored depth of 15.75 m. The N values observed at the location varied from 22 (at 3.30 m depth) to 38 (at 15.30 m depth). Similarly, from figure 3b, it can be seen that the subsurface soil at the location of bridge 1274/1 predominantly consists of clay with medium compressibility (CI) and to some extent contains clay with low compressibility (CL) and intermediate silt (ML). The N values observed at the site varied from 14 (at 1.80 m depth) to 38 (at 15.30 m depth). The groundwater table was not encountered in any of the bridge locations during the field exploration. Figures 4 and 5 show the typical gradation curves for the soil collected from various depths of the boreholes at different bridge sites. The p–q plots were established by performing UU triaxial tests on the undisturbed soil samples collected from multiple depths of the boreholes and the undrained shear strength parameters (c_u and ϕ_u) determined from the respective p–q plots are reported in figure 3.

At both of the bridge locations, plate load test was performed as per the procedure laid down in the Indian standard specification [18]. From the pressure–settlement curve obtained from the plate load test conducted at the location of bridge 1273/1 (figure 6a), it can be observed that the curve follows a conventional and steady-state increasing trend when the pressure on the test plate reaches up to 70.77 t/m^2 (694.02 kPa) with a total settlement of 14.54 mm. Adopting the double tangent method, the

Location (Bridge No.1273/1)	Depth(m)	S.P.T				Partical Size Analysis							IS Classification	Natural Bulk Density (gm/cc)	Natural water Content	U-U Triaxial Shear Test Results/Direct Shear Test		Consolidation Test	
		Observed 'N' value	Sampling	Liquid Limit, %	Plasticity Index	Clay% (<0.002mm)	Silt % (0.002-0.075mm)	Sand % (0.075-4.75mm)	Gravel% (>4.75mm)	D_{10} (mm)	D_{30} (mm)	D_{60} (mm)				Cohesion 'c,' kg/cm^2	Angle Of Friction 'Φu'	Initial Void ratio e_0	Compression Index C_c
	GL																		
Silty Clay	1.50-1.80		*UDS	34	11	19	63	9	10	-	0.0095	0.043	CL	1.54	9.06	0.6	8.5	0.87	0.16
Silty Clay/ Clayey silt	1.80-2.25	24	*SPT	37	18	11	76	10	3	-	0.0190	0.050	CI						
	3.00-3.30		UDS	31	8	11	73	13	3	0.0017	0.0230	0.059	CL	1.49	3.6	0.18	22	0.83	0.18
Silty Clay	3.30-3.75	22	SPT	30	8	7	73	12	9	0.0060	0.0240	0.061	CL						
Silty Clay	4.50-4.80		UDS	33	12	4	74	14	8	0.0078	0.0290	0.065	CL	1.49	5.9	0.58	20	0.87	0.19
Silty Clay/ Clayey silt	4.80-5.25	24	SPT	41	21	24	67	3	5	-	0.0032	0.036	CI						
	6.00-6.30		UDS	37	16	13	62	10	16	0.0017	0.0180	0.055	CI	1.57	11.3	0.26	5.2	0.87	0.17
Clayey silt	6.30-6.75	27	SPT	35	10	2	85	13	0	0.0058	0.0280	0.050	MI						
Silty Clay	7.50-7.80		UDS	32	10	9	65	7	20	0.0030	0.0310	0.061	CL	1.71	14.8	0.36	10	0.76	0.13
Clayey silt	7.80-8.25	25	SPT	34	9	0	84	10	6	0.0280	0.0360	0.059	ML						
Silty Clay/ Clayey silt	9.00-9.30		UDS	39	17	10	79	8	3	0.0021	0.0210	0.050	CI	1.74	13.3	0.52	8	0.71	0.16
	9.30-9.75	28	SPT	40	23	13	83	4	1	0.0012	0.0170	0.040	CI						
	10.50-10.80		UDS	36	17	12	79	8	1	-	0.0250	0.050	CI	2.06	13.5	0.7	4	0.45	0.11
	10.80-11.25	27	SPT	36	15	15	78	5	1	-	0.0160	0.041	CI						
Silty Clay/ Clayey silt	12.00-12.30		UDS	35	16	11	80	7	3	-	0.0270	0.050	CI	2.14	15.9	0.33	4	0.43	0.11
	12.30-12.75	30	SPT	34	14	14	82	4	1	-	0.0160	0.042	CL						
Silty Clay/ Clayey silt	13.50-13.80		UDS	36	17	13	81	4	2	-	0.0210	0.045	CI	1.97	13.1	0.68	5	0.52	0.13
	13.80-14.25	33	SPT	36	18	20	73	6	1	-	0.0140	0.042	CI						
Silty Clay	15.00-15.30		*DS	29	8	7	71	20	2	0.0050	0.0280	0.061	CL						
	15.30-15.75	38	SPT	30	9	5	74	19	2	0.0061	0.0280	0.061	CL						

Note: *UD-Undisturbed Sample , *SPT- Standard Penetration Test , *DS-Disturbed Sample

(a)

Location (Bridge No.1274/1)	Depth(m)	S.P.T				Partical Size Analysis							IS Classification	Natural Bulk Density (gm/cc)	Natural water Content	U-U Triaxial Shear Test Results/Direct Shear Test		Consolidation Test	
		Observed 'N' value	Sampling	Liquid Limit, %	Plasticity Index	Clay% (<0.002mm)	Silt % (0.002-0.075mm)	Sand % (0.075-4.75mm)	Gravel% (>4.75mm)	D_{10} (mm)	D_{30} (mm)	D_{60} (mm)				Cohesion 'c,' kg/cm^2	Angle Of Friction 'Φu'	Initial Void ratio e_0	Compression Index C_c
	GL																		
Silty Clay/ Clayey silt	1.50-1.80		*UDS	36	17	11	51	32	6	0.0015	0.032	0.07	CI	1.8	7.3	0.74	11	0.57	0.08
Silty Clay	1.80-2.25	14	*SPT	31	14	15	48	30	7	-	0.019	0.068	CL						
Clayey silt	3.00-3.30		UDS	34	10	2	89	9	0	0.01	0.03	0.051	ML	1.63	9.6	0.49	23	0.77	0.15
Silty Clay/ Clayey silt	3.30-3.75	16	SPT	35	17	20	73	7	1	-	0.0095	0.041	CI						
	4.50-4.80		*DS	39	15	24	70	6	0	-	0.0045	0.038	CI	1.97	18.6	0.22	0	0.58	
Clayey silt	4.80-5.25	17	SPT	34	9	4	90	6	0	-	0.025	0.048	ML						
Silty Clay/ Clayey silt	6.00-6.30		DS	37	19	15	75	9	1	-	0.019	0.041	CI	1.91	16.2	1.84	5.4	0.6	0.14
	6.30-6.75	27	SPT	35	15	18	69	9	4	-	0.0096	0.04	CI						
	7.50-7.80		DS	35	16	26	63	10	1	-	0.0042	0.036	CI	2.07	17.3	0	22	0.49	0.12
Silty Clay	7.80-8.25	32	SPT	32	12	11	80	7	1	0.0017	0.017	0.041	CL						
Silty Clay/ Clayey silt	9.00-9.30		DS	38	15	15	71	12	2	-	0.017	0.049	CI	1.99	14	0.64	7	0.51	0.13
	9.30-9.75	20	SPT	36	17	15	72	11	2	-	0.016	0.05	CI						
Silty Clay/ Clayey silt	10.50-10.80		DS	36	18	12	62	17	9	0.0019	0.011	0.06	CI						
	10.80-11.25	29	SPT	38	19	16	58	17	9	-	0.0089	0.039	CI						
Silty Clay/ Clayey silt	12.00-12.30		DS	38	19	11	67	16	7	0.002	0.015	0.05	CI	2.03	18.7	0.63	16	0.54	0.12
	12.30-12.75	36	SPT	38	18	13	65	15	7	0.0015	0.013	0.055	CI						
Silty Clay/ Clayey silt	13.50-13.80		DS	38	20	16	63	15	6	-	0.013	0.045	CI	1.97	18.7	0.32	10	0.58	0.12
	13.80-14.25	37	SPT	39	18	17	72	9	2	-	0.0055	0.018	CI						
Silty Clay/ Clayey silt	15.00-15.30		DS	37	16	17	53	16	14	-	0.017	0.062	CI						
	15.30-15.75	38	SPT	38	17	16	57	15	12	-	0.017	0.062	CI						

Note: *UD-Undisturbed Sample , *SPT- Standard Penetration Test , *DS-Disturbed Sample

(b)

Figure 3. Bore-log data at the location of (**a**) 1273/1 and (**b**) 1274/1 (modified after Ghosh and Chandra (2016) [17]).

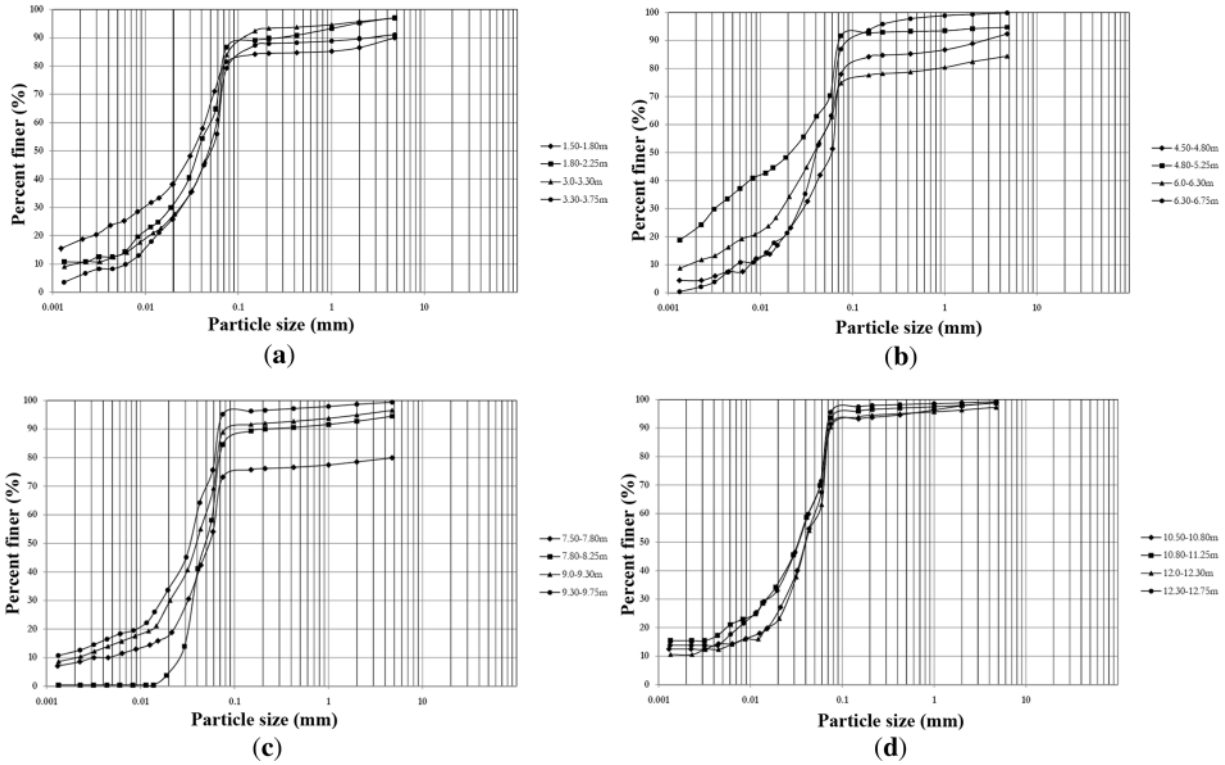

Figure 4. Typical gradation curves for different depths at the location of 1273/1 (modified after Ghosh and Chandra (2016) [17]).

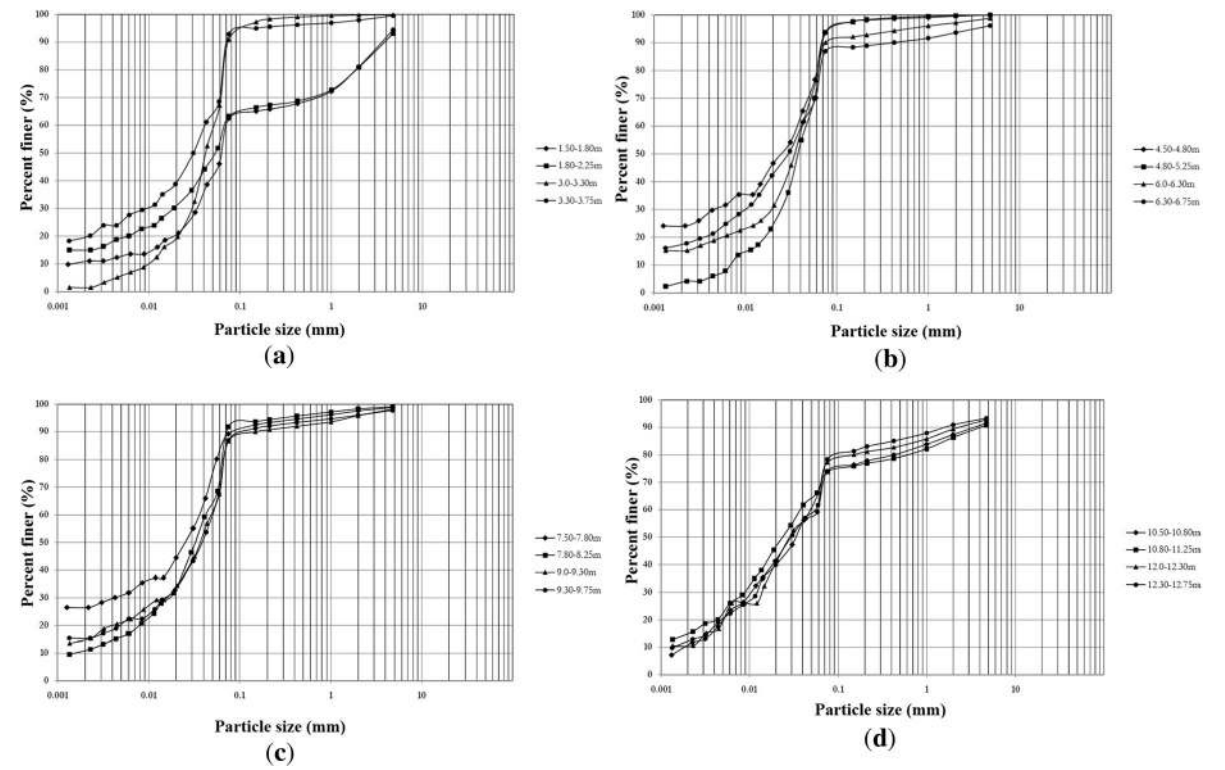

Figure 5. Typical gradation curves for different depths at the location of 1274/1 (modified after Ghosh and Chandra (2016) [17]).

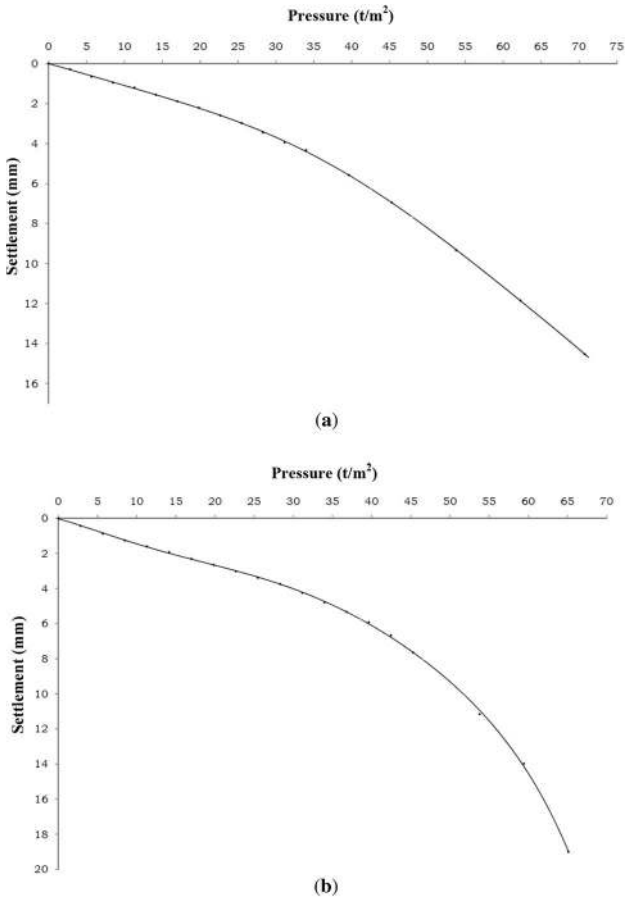

Figure 6. Pressure–settlement curve from plate load test at the location of (**a**) 1273/1 and (**b**) 1274/1 (modified after Ghosh and Chandra (2016) [17]).

ultimate bearing capacity can be determined as 37.5 t/m^2 (367.75 kPa). The moisture content of the soil below the test plate was estimated as 15.54% on the day of conducting the plate load test. Similarly, from the pressure–settlement plot obtained at the location of bridge 1274/1 (figure 6b), it can be noted that the curve follows a conventional and steady-state increasing trend when the pressure on the test plate reaches up to 65.11 t/m^2 (638.51 kPa) with a total settlement of 19.01 mm. Considering the double tangent method, the ultimate bearing capacity can be obtained as 51 t/m^2 (500.14 kPa). The moisture content of the soil below the test plate was estimated as 16.12% on the day of conducting the plate load test. Based on the information provided by the Rail Vikas Nigam Limited (RVNL), Kanpur, India, the design load intensity was considered as 15 t/m^2 (147.1 kPa). From the pressure–settlement curves obtained from the plate load test performed at different bridge locations, the net safe bearing capacity was found to be more than 147.1 kPa, considering a factor of safety equal to 2.5. Hence, keeping the design load intensity (147.1 kPa) in consideration, both locations were found to be safe as far as the plate load test was concerned.

3. Materials

The existing bridges consist of super- and sub-structure made of brick masonry. The different strength properties of the foundation soil for bridges 1273/1 and 1274/1 have been extracted from the bore-log data given in figure 3 and are reported in tables 1 and 2, respectively. The bridges carry a layered earth embankment throughout, whose properties are provided by the RVNL. The details of the embankment for both the existing and the proposed bridges are shown in figure 7. The embankment generally consists of three layers, i.e., blanket, SQ2 and SQ1 as shown in figure 7. The depth of different layers (blanket, SQ2 and SQ1) of the embankment was provided by the RVNL. It has been reported by several investigators that the performance of the railway track is highly dependent on the different components such as rails, ballasts and sleepers [19, 20]. The material properties of the different components of the existing bridge, the track and the embankment are given in tables 3 and 4 for bridges 1273/1 and 1274/1, respectively, whereas the soil properties are determined using the empirical correlations recommended by Das [21]. The elastic modulus of the different layers (blanket, SQ2 and SQ1) of the embankment is determined using the following expression:

$$E = \beta S_{\mathrm{u}} \tag{1}$$

where S_{u} is the undrained shear strength of the soil. The magnitude of the coefficient β has been determined from the chart proposed by Das [21]. The different values of β for the blanket, SQ2 and SQ1 are found to be 1175, 1125 and 570, respectively.

The Poisson's ratio (υ) for the soil has been determined using the following expression [22, 23]:

$$\upsilon = \begin{matrix} 0.25 + 0.00225(\mathrm{PI}) : \text{for clayey soil} \\ 0.1 + 0.3\left(\dfrac{\phi_{\mathrm{d}} - 25}{45^0 - 25^0}\right) : \text{for granular soil} \end{matrix} \tag{2}$$

where ϕ_{d} is the drained angle of internal friction of the soil.

4. FE modelling

A schematic diagram of the existing bridges with dimensions is shown in figure 2, as furnished by the RVNL. The length of the existing old bridge 1273/1 is 30.15 m and that of the newly proposed bridge is 13.291 m; thus the total length of the bridge becomes 43.441 m. The length of the existing old bridge 1274/1 is 37 m, and that of the newly proposed bridge is 18.757 m; thus the total length of the bridge becomes 55.757 m. The FE analysis of the bridge as well as the soil system has been performed using a commercially available FE software ABAQUS/CAE 6.13-4. Eight noded linear brick elements with reduced integration (C3D8R) have been adopted to model the bridge and the soil system since a good mesh of hexahedral elements

Table 1. Strength properties of soil at the location of bridge 1273/1.

Layer no.	Depth (m)	Unit weight (kN/m^3)	c_u (kN/m^2)	ϕ_u (deg)	Stress (kPa)	S_u (kPa)	Elastic modulus (MPa)	PI	Poisson's ratio (ν)
1	3.00	15.11	58.84	8.5	22.66	62.23	59.74	18	0.29
2	4.50	14.62	17.65	22	56.28	40.39	50.89	8	0.27
3	6.00	14.62	56.88	20	78.21	85.34	74.25	21	0.30
4	7.50	15.40	25.50	5.2	100.72	34.66	35.36	16	0.29
5	9.00	16.78	35.30	10	124.86	57.32	68.78	10	0.27
6	10.50	17.07	50.99	8	150.24	72.11	58.41	23	0.30
7	12.00	20.21	68.65	4	178.20	81.11	80.30	17	0.29
8	13.50	20.99	32.36	4	209.10	46.98	47.92	16	0.29

Table 2. Strength properties of soil at the location of bridge 1274/1.

Layer no.	Depth (m)	Unit weight (kN/m^3)	c_u (kN/m^2)	ϕ_u (deg)	Stress (kPa)	S_u (kPa)	Elastic modulus (MPa)	PI	Poisson's ratio (ν)
1	3.00	17.66	72.57	11	26.49	77.72	76.94	17	0.29
2	4.50	15.99	48.05	23	64.97	75.63	74.87	17	0.29
3	6.00	19.33	21.57	0	91.45	21.57	22.65	15	0.28
4	7.50	18.74	180.44	5	120.00	191.79	178.36	19	0.29
5	9.00	20.31	0.00	22	149.28	60.31	61.52	16	0.29
6	10.50	19.52	62.76	7	179.16	84.76	83.91	17	0.29
7	12.00	Disturbed sample was obtained and hence the properties are considered same as those of layer no. 6.							
8	13.50	19.82	61.78	16	237.94	130.01	124.81	18	0.29

(C3D8R) usually provides a solution of equivalent accuracy at less cost. The details of the FE meshing for the existing bridge are given in figure 8. The foundation of the bridges is assumed to rest on the soil surface. The interface between the soil and the foundation is considered as perfectly rough. After performing a sensitivity analysis, the dimensions of the soil domain for bridges 1273/1 and 1274/1 have been chosen as 80 m × 55 m and 80 m × 50 m along the x and z directions, respectively (figure 8). The depth of the soil deposit along the y direction is kept fixed at 13.5 m. The base of the soil is kept fixed in all three directions, and the sides of the soil domain are allowed to move only in the vertical direction using the roller support. However, for the embankment, only the sides along the x–y plane are restrained with the roller support to move only in the vertical direction. In the analysis, the embankment is considered to behave as linearly elastic. The stress–strain behaviour of the soil in the current analysis is satisfactorily assumed to be linearly elastic.

A 3D FE model developed for the newly proposed bridge along with the existing bridge is shown in figure 9. The boundary conditions are kept similar to those of the model developed for the existing bridge. For bridges 1273/1 and 1274/1, the length of the soil domain is kept as 90 and 100 m, respectively, to accommodate the extension due to the proposed structure. However, the width and the depth of the domain are kept same as those of the model developed for the existing bridge. The discretization of the ballast, the track and the soil has been carried out using C3D8R elements, whereas the embankment has been discretized using C3D4 elements available in ABAQUS. It is worth noting that C3D4 is a general purpose tetrahedral element with four nodes and one integration point. As the embankment continues along the z direction on either side of the bridge, an equivalent surcharge is considered at the ground level for both the existing as well as the proposed bridge.

5. Train loading

The span between Kanpur Central and Parichha (25.5188°N, 78.7383°E), near Jhansi Junction, is designated as the feeder route of the dedicated freight corridor (DFC) by the IR on which heavy axle trains are expected to travel for feeding coal to the Parichha Thermal Power Station. Hence, in the present analysis, the train loading has been considered as DFC 32.5 t for all the tracks as reported by Chakrabarti [24], which has been recommended by the IR for the dedicated freight corridor. Detailed discussion on

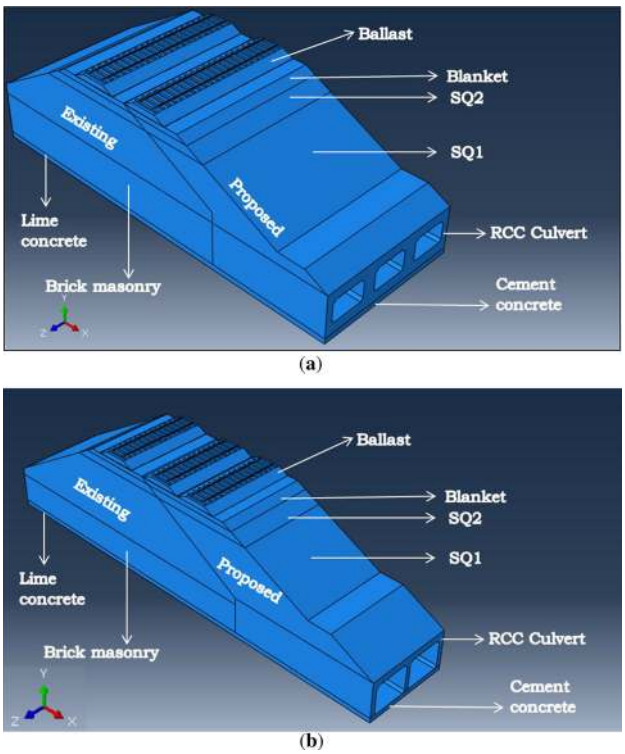

Figure 7. Details of the embankment for (**a**) 1273/1 and (**b**) 1274/1.

Table 3. Material properties of different components of bridge, track and embankment for bridge 1273/1.

Material	Properties		
	Density (kg/m^3)	Elastic modulus (MPa)	Poisson's ratio
Brick masonry	1700	2500	0.2
Ballast	1800	30.49	0.15
Blanket	1960	13.22	0.15
SQ2	1860	27.91	0.32
SQ1	1810	39.11	0.295
Lime/cement concrete	2400	2.5×10^4	0.2
Steel rail	7477	2.1×10^5	0.3
Sleeper	2756	3.845×10^4	0.2

the DFC loading is not repeated in this paper, for which the report of Chakrabarti [24] can be referred. However, the details of the DFC 32.5 t loading are schematically shown in figure 10, where the axel loadings as well as the distance between the axle loadings for both diesel loco and wagons are clearly demonstrated. The rail loads are applied as quasi-static point loads on the existing as well as the newly proposed tracks. The applied axle loads have been made double considering the dynamic factor.

Table 4. Material properties of different components of bridge, track and embankment for bridge 1274/1.

Material	Properties		
	Density (kg/m^3)	Elastic modulus (MPa)	Poisson's ratio
Brick masonry	1700	2500	0.2
Ballast	1800	30.49	0.15
Blanket	1960	13.22	0.15
SQ2	1860	27.91	0.32
SQ1	1810	85.81	0.295
Lime/cement concrete	2400	2.5×10^4	0.2
Steel rail	7477	2.1×10^5	0.3
Sleeper	2756	3.845×10^4	0.2

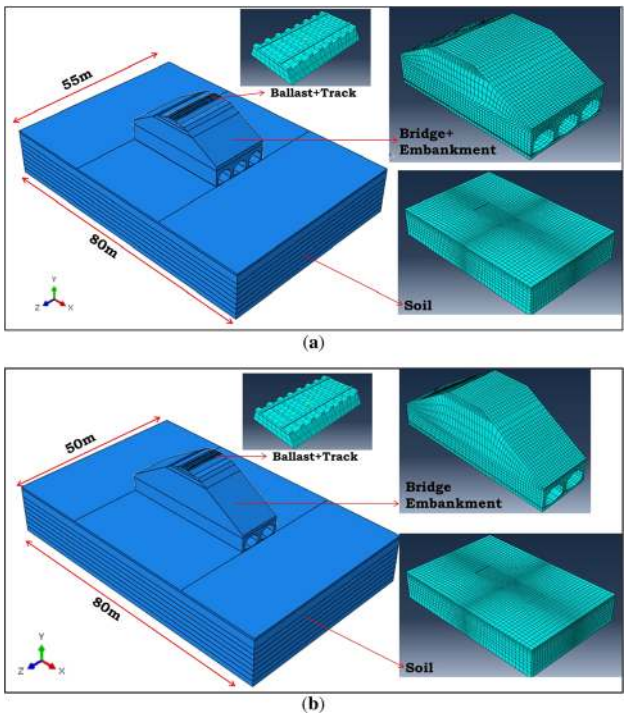

Figure 8. 3D FE model and discretization of the existing bridge: (**a**) 1273/1 and (**b**) 1274/1.

6. Results and discussion

The computation time needed for the whole analysis typically ranges from 9 to 14 min depending upon the number of elements present in the model. For bridge 1273/1, three typical sections have been selected for determining the vertical stress and the settlement distribution developed below the foundation (figure 11a). Section-AA represents the section along the centreline of the existing track. Section-BB represents the edge (end) of the existing bridge, i.e., the junction between the existing and the proposed

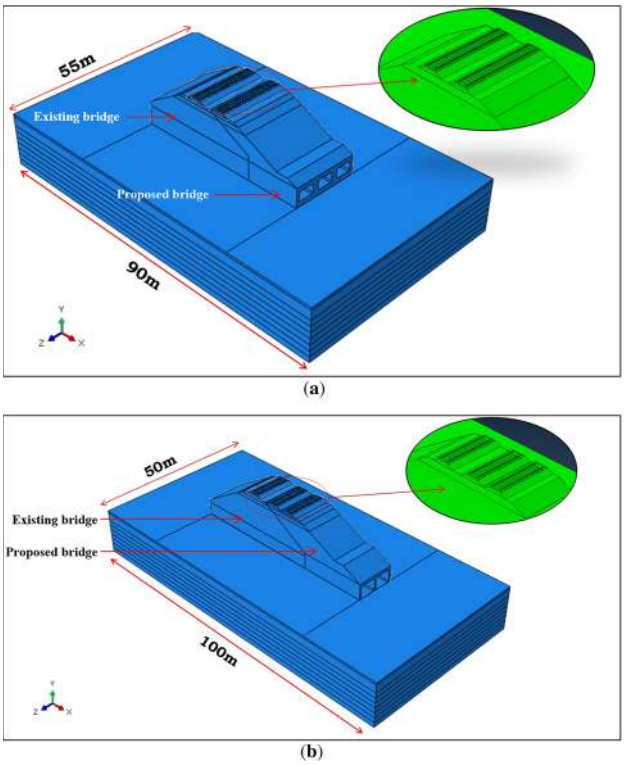

Figure 9. 3D FE model of the proposed bridge along with the existing bridge: (**a**) 1273/1 and (**b**) 1274/1.

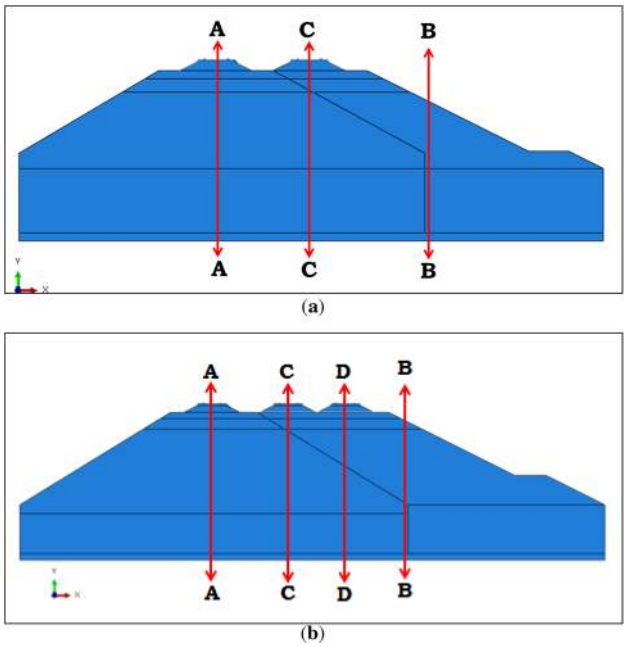

Figure 11. Selected sections to determine vertical stress and settlement for (**a**) 1273/1 and (**b**) 1274/1.

bridge. Section-CC represents the section along the centreline of the proposed track as shown in figure 11a. Similarly, for bridge 1274/1, four typical sections have been selected for obtaining the vertical stress and the settlement distribution developed below the foundation (figure 11b). Section-AA represents the section along the centreline of the existing track. Section-BB represents the edge (end) of the existing bridge, i.e. the junction between the existing and the proposed bridge. Section-CC and section-DD represent the sections along the centreline of the two proposed tracks as shown in figure 11b. The analysis has been

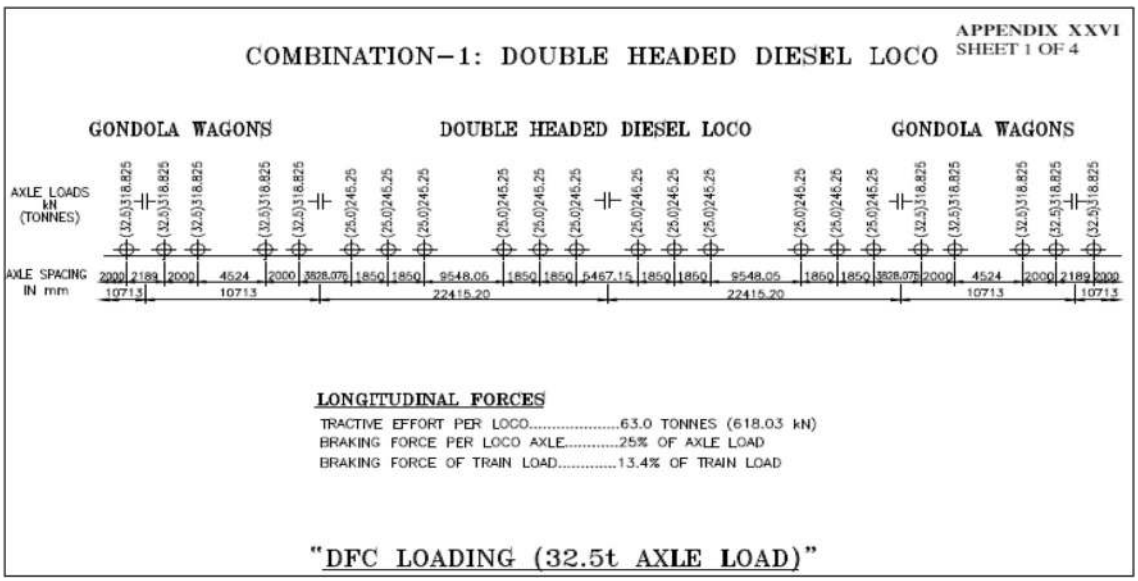

Figure 10. Loading standards for DFC loading (modified after Chakrabarti (2016) [24]).

Table 5. Maximum vertical stress and settlement at different sections at different loading conditions for bridge 1273/1.

Section		AA		BB		CC	
Loads		Only DL	DL + train load	Only DL	DL + train load	Only DL	DL + train load
Existing: 1273/1	Maximum vertical stress (kPa)	180.8	201.3	120.9	129.6	172.5	189.4
	Maximum settlement (mm)	26.23	29.03	21.94	23.76	25.14	27.56
Proposed: 1273/1 (considering train load on both tracks)	Maximum vertical stress (kPa)	188.7	219.2	154.0	168.4	190.1	219.8
	Maximum settlement (mm)	27.62	32.03	25.04	27.82	27.51	31.70

Table 6. Maximum vertical stress and settlement at different sections at different loading conditions for bridge 1274/1.

Section		AA		BB		CC		DD	
Loads		Only DL	DL + train load	Only DL	DL + train load	Only DL	DL + train load	Only DL	DL + train load
Existing: 1274/1	Maximum vertical stress (kPa)	217.4	241.9	141.5	149.9	198.8	217.4	172.6	185.5
	Maximum settlement (mm)	25.59	28.34	17.85	19.08	24.28	26.58	21.52	23.22
Proposed: 1274/1 (considering train load on both tracks)	Maximum vertical stress (kPa)	239.3	288.8	171.3	197.3	261.5	322.8	233.7	281.7
	Maximum settlement (mm)	27.88	33.57	25.25	29.14	28.58	34.92	27.07	32.54

performed in two different stages. In the first stage, the structure has been analysed considering only the dead load (DL), whereas in the second stage, the train load (live load) has been applied on the track. The magnitude of the maximum vertical stress and the settlement developed below the foundation at the selected sections is tabulated in tables 5 and 6 for bridges 1273/1 and 1274/1, respectively. In this case study, the occurrence of interaction between the foundations of existing and proposed bridge is quite obvious due to close spacing. For bridge 1273/1, the maximum vertical stress at section-AA is observed to increase from 201.3 to 219.2 kPa, resulting in about 8.93% increase due to the placement of the proposed railway track. Section-BB is found to be critical as it serves as the junction between the existing and the proposed bridges. The analysis shows an increase in the maximum vertical stress from 129.6 to 168.4 kPa at section-BB, i.e. 29.91% increase due to the placement of the proposed railway track. Similarly, the maximum settlement at section-AA and section-BB is observed to increase from 29.03 to 32.03 and from 23.76 to 27.82 mm, respectively, resulting in about 10.33% and 17.09% increase due to the placement of the proposed railway track. The maximum vertical stress and the settlement at section-CC is found to increase from 189.4 to 219.8 kPa and from 27.56 to 31.7 mm, respectively, resulting in about 16.07% and 15.02% increase due to the placement of the proposed railway track. After placement of the proposed bridge, among all the three sections (AA, BB and CC), the maximum difference in the settlement between only DL condition and DL plus train load condition is found to be 6.56 mm (31.7–25.14 mm = 6.56 mm), which occurs at section-CC. This value is well within the permissible settlement limit of 25 mm, as per the IR Standard code (IR Standard 2013). On the contrary, for bridge 1274/1, the maximum vertical stress at section-AA is observed to increase from 241.9 to 288.8 kPa, resulting in about 19.38% increase due to the placement of the proposed railway track. Section-BB is found to be critical as it serves as the junction between the existing and the proposed bridges. The analysis shows an increase in the

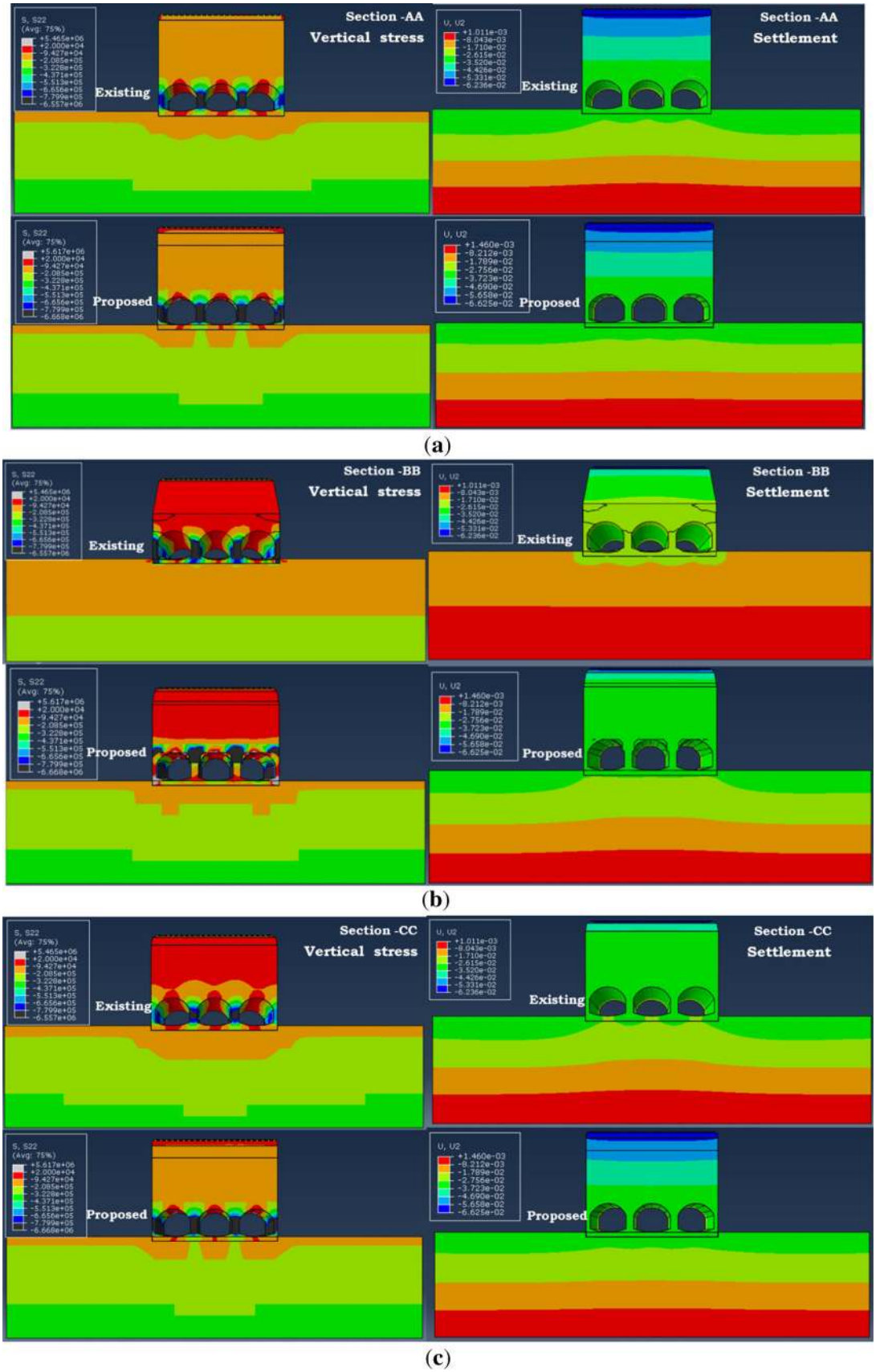

Figure 12. Vertical stress and settlement distribution for 1273/1 at section (**a**) AA, (**b**) BB and (**c**) CC.

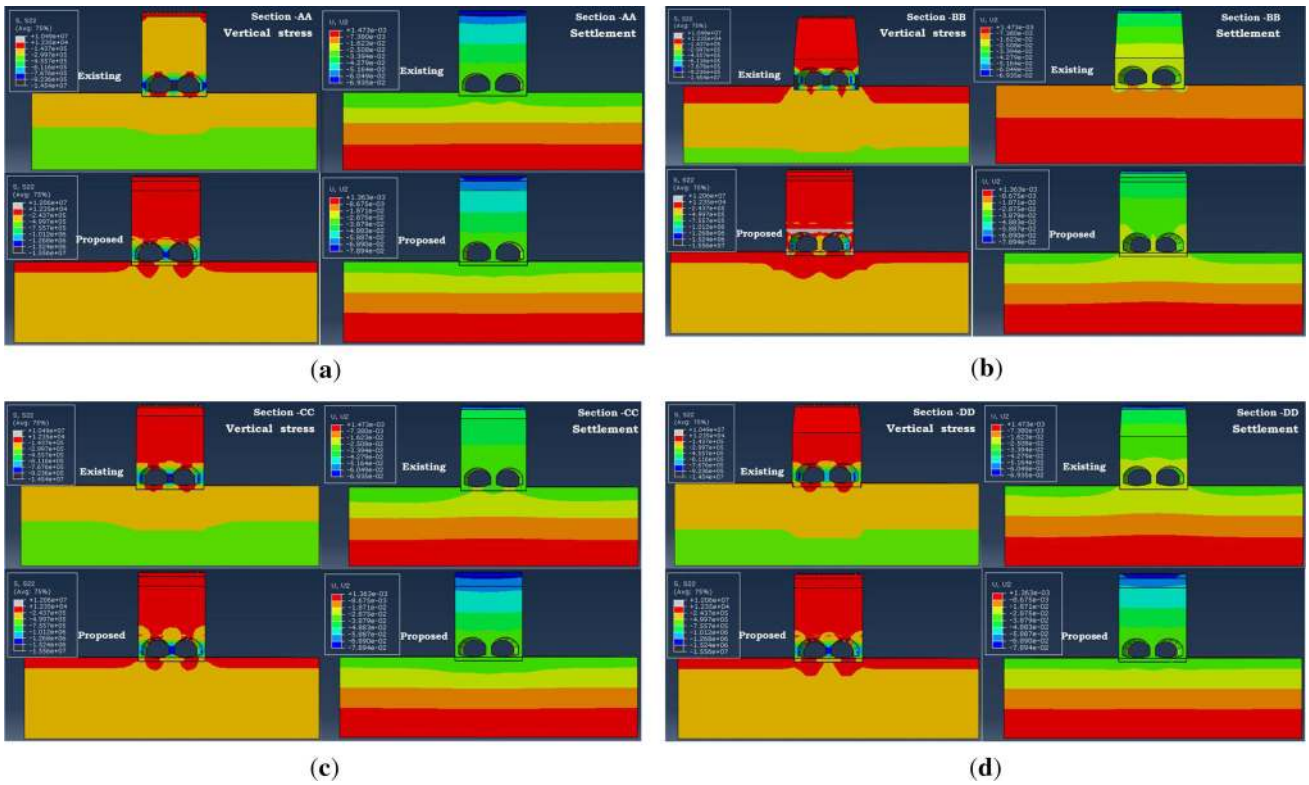

Figure 13. Vertical stress and settlement distribution for 1274/1 at section (**a**) AA, (**b**) BB, (**c**) CC and (**d**) DD.

maximum vertical stress from 149.9 to 197.3 kPa at section-BB, i.e., 31.64% increase due to the placement of the proposed railway track. Similarly, the maximum settlement at section-AA and section-BB is observed to increase from 28.34 to 33.57 and from 19.08 to 29.14 mm, respectively, resulting in about 18.45% and 52.72% increase due to the placement of the proposed railway track. The maximum vertical stress and the settlement at section-CC are found to increase from 217.4 to 322.8 kPa and from 26.58 to 34.92 mm, respectively, resulting in about 48.5% and 31.37% increase due to the placement of the proposed railway track. Similarly, the maximum vertical stress and the settlement at section-DD is found to increase from 185.5 to 281.7 kPa and from 23.22 to 32.54 mm, respectively, resulting in about 51.88% and 40.14% increase due to the placement of the proposed railway track. After placement of the proposed bridge, among all the four sections (AA, BB, CC and DD), the maximum difference in the settlement between only DL condition and DL plus train load condition is found to be 11.29 mm (29.14–17.85 mm = 11.29 mm), which occurs at section-BB. This value is well within the permissible settlement limit of 25 mm, as per the IR Standard code [25].

Under the combined effect of the DL and the train load, the contour plots of the vertical stress and the settlement distribution at different sections of bridges 1273/1 and 1274/1 in the presence of the existing as well as the proposed structure are shown in figures 12 and 13, respectively. It can be observed from the contour plots depicted in figures 12 and 13 that the vertical stress and the settlement developed below the foundation of the existing bridge get significantly enhanced by the placement of the proposed bridge.

7. Conclusions

In the present study, the geotechnical stability of the substructure of more than 100-year-old brick masonry arch bridges has been analysed numerically due to the construction of the adjacent newly proposed concrete box bridges. Two different bridges (1273/1 and 1274/1) have been considered in this analysis. Bridge 1273/1 is made of brick masonry with three barrels, whereas bridge 1274/1 is made of brick masonry with two barrels. For bridges 1273/1 and 1274/1, the maximum vertical stress developed at the base of the foundation of the existing bridge in the presence of the proposed bridge is found to be 219.83 and 322.83 kPa, respectively, which is significantly lower than the ultimate bearing capacity (367.75 and 500.14 kPa, respectively) obtained at the respective bridge locations. After placement of the proposed bridge, among all the selected sections, the maximum difference in the settlement between only DL condition and DL plus train load condition is found to be

6.56 and 11.29 mm for bridges 1273/1 and 1274/1, respectively, which is well within the permissible settlement limit of 25 mm. Hence, both of the existing bridges may be considered to be safe with respect to the strength and the serviceability criteria of the foundation.

Acknowledgements

The authors are thankful for the financial support provided by the Rail Vikas Nigam Limited (RVNL), Kanpur, India, to carry out the present work through a sponsored project [Ref No. 42/CPM/RVNL/CNB/2015/44].

References

[1] Bowles J E 1977 *Foundation analysis and design*. New York, USA: McGraw-Hill

[2] Das B M and Larbi-Cherif S 1983 Bearing capacity of two closely-spaced shallow foundations on sand. *Soils and Foundations* 23(1): 1–7

[3] Das B M, Puri V K and Neo B K 1993 *Interference effects between two surface footings on layered soil.* Transportation Research Record 1406, Transportation Research Board, Washington, DC, pp. 34–40

[4] Ghosh P and Kumar S R 2011 Interference effect of two nearby strip surface footings on cohesionless layered soil. *International Journal of Geotechnical Engineering* 5(1): 87–94

[5] Griffiths D V, Fenton G A and Manoharan N 2006 Undrained bearing capacity of two strip footings on spatially random soil. *International Journal of Geomechanics* 6(6): 421–427

[6] Kumar J and Bhoi M K 2009 Interference of two closely spaced strip footing on sand using model test. *Journal of Geotechnical and Geoenvironmental Engineering* 135(4): 595–604

[7] Kumar J and Ghosh P 2007 Ultimate bearing capacity of two interference rough strip footings. *International Journal of Geomechanics* 7(1): 53–62

[8] Kumar J and Ghosh P 2007 Upper bound limit analysis for finding interference effect of two nearby strip footing on sand. *Geotechnical and Geological Engineering* 25(5): 499–507

[9] Kumar J and Kouzer K M 2007 Bearing capacity of two interfering footings. *International Journal for Numerical Analytical Methods in Geomechanics* 32(3): 251–264

[10] Lavasan A A, Ghazavi M, von Blumenthal A and Schanz T 2018 Bearing capacity of interfering strip footings. *Journal of Geotechnical and Geoenvironmental Engineering* 144(3): 04018003

[11] Saran S and Agarwal V C 1974 Interference of surface footings on sand. *Indian Geotechnical Journal* 4(2): 129–139

[12] Selvadurai A P S and Rabbaa S A A 1983 Some experimental studies concerning the contact stresses beneath interfering rigid strip foundations resting on a granular stratum. *Canadian Geotechnical Journal* 20(3): 406–415

[13] Stuart J G 1962 Interference between foundations, with special reference to surface footings in sand. *Geotechnique* 12(1): 15–22

[14] West J M and Stuart J G 1965 Oblique loading resulting from interference between surface footings on sand. In: *Proceedings of the 6th International Conference on Soil Mechanics and Foundation Engineering*, Montreal, vol. 2, pp. 214–217

[15] Perloff W H 1975 Pressure distribution and settlement. In: *Foundation engineering handbook*

[16] IS 2131 – 1981 (reaffirmed 2002) 2002 Method for standard penetration test for soils. 1st Revision, Bureau of Indian Standards, Manak Bhavan, New Delhi, India

[17] Ghosh P and Chandra S 2016 *Geotechnical investigations for seven old arch bridges in connection with doubling of tracks between Kanpur and Jhansi*. Report No. CE/GTE/PG/2016/420, September 29

[18] IS 1888 – 1982 (reaffirmed 2002) 2002 *Method of load test on soils*. 2nd Revision, Indian Standards Institution, Manak Bhavan, New Delhi, India

[19] Laryea S, Safari Baghsorkhi M, Ferellec J F, McDowell G R and Chen C 2014 Comparison of performance of concrete and steel sleepers using experimental and discrete element methods. *Transportation Geotechnics* 1: 225–240

[20] Shahraki M, Warnakulasooriya C and Witt K J 2015 Numerical study of transition zone between ballasted and ballastless railway track. *Transportation Geotechnics* 3: 58–67

[21] Das B M 1997 *Advanced soil mechanics*. London, UK: Taylor and Francis

[22] Trautmann C H and Kulhawy F H 1987 *CUFAD—a computer program for compression and uplift foundation analysis and design*. Report EL-4540-CCM, 16, Electrical Power and Research Institute

[23] Wroth C P 1975 In situ measurement of initial stresses and deformation characteristics. In: *Proceedings of the Specialty Conference on In Situ Measurement of Soil Properties*, vol. 2, pp. 180–230

[24] Chakrabarti S K 2016 *Evaluation of structural adequacy of bridge no. 1130/2 and its strengthening for the doubling of track between Kanpur and Jhansi (structural-scope only)*, Kanpur

[25] Indian Railway Standard (IRS) 2013 *Code of practice for the design of sub-structures and foundations of bridges*. 2nd Revision, Research Designs and Standards Organisation, Lucknow, India